

Pulse Rate Estimation Using Hydraulic Bed Sensor

B.Y. Su, K.C. Ho, M. Skubic, and L. Rosales

Abstract—We propose in this paper an effective method to obtain the pulse rate from a hydraulic sensor that is placed under the mattress. The sensor captures the superposition of the ballistocardiogram (BCG) and the respiration signals. The BCG is modeled as the j-peak with a frequency modulation component. The proposed method utilizes the Hilbert transform to effectively capture the j-peak, which allows the pulse rate information to come out distinctively in the frequency domain. Among the five subjects tested, the error in pulse rate estimation is less than 1%.

I. INTRODUCTION

In the United States, cardiovascular disease affects 37% of the population [1]. In-home pulse rate monitoring systems can provide early signs of the problem and avoid fatal consequences. We are interested in monitoring the pulse rate of a person while sleeping. Although many types of wireless wearable pulse rate sensors have been developed, non-wearable monitoring system are more comfortable for sleeping.

Previous non-invasive sensor systems for pulse rate monitoring include an image-based system [2], ultrasonic sensor [3] [4], mattress type sensor [5] and infrared diode sensor [6]. They are, however, expensive and complicated. The pillow type sensor [7] is easy to install and maintain. However, it does not often provide consistent signal measurements.

In this paper, we use a hydraulic sensor for pulse rate monitoring. It is composed of a tube filled with water and a pressure sensor. The sensor is placed under the mattress to maintain the sleeping comfort.

The data acquired from the sensor contains the BCG [8] and the respiration signals. After removing the respiration component, the Hilbert transform [9][10] is applied to extract the pulse envelopes from which the pulse rate is estimated. Compared with previous methods [11] [12], better estimation accuracy is achieved.

This paper is organized as follows. The details of the hydraulic bed sensor and measurement parameters are described in section II. In section III, the approach of using the Hilbert transform for pulse rate estimation is presented. The estimation algorithm is developed in section IV. The results are given in section V. Finally, the conclusion will be drawn in section VI.

B.Y.Su and L. Rosales are with the ECE Dept., University of Missouri (e-mail: bsdg6@mail.missouri.edu, lr5zf@mail.missouri.edu).

K.C.Ho and M.Skubic are with the ECE Dept., University of Missouri (e-mail: HoD@missouri.edu, SkubicM@missouri.edu).

TABLE I

DETAILS OF PARTICIPANTS FOR EVALUATION.

Subject	Gender	Age	Height (cm)	Weight (kg)	Cardiac history
1	male	24	180	86	No
2	male	26	170	63	No
3	female	30	160	58	No
4	female	32	163	53	Yes
5	male	32	173	86	No

II. THE HYDRAULIC BED SENSOR

The transducer is a three inch wide, twenty inch long discharged hose that is filled with 70 percent of water. The end of the transducer has an integrated silicon pressure sensor (Freescale MPX5010GP) that is used for measuring the vibration from the discharged hose. In the experimental setup, four sensors are placed under the mattress as shown in Fig. 1 (a). The output signal of the integrated pressure sensor is connected to the hardware filtering circuit. The hardware filtering circuit is composed of an amplifier and a filter. The amplifier uses 741 op-amp to amplify the signal by the factor of 10. The filter is an 8th-order integrated Bessel filter (Maxim MAX7401). The signal is sampled by the National Instruments NI9201 12-bit analog to digital converter (ADC) with a sampling rate equal to 100 Hz. The typical pulse obtained from the sensor is shown in Fig. 1 (b).

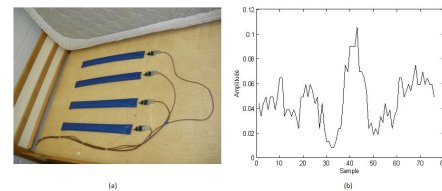


Fig. 1. (a)Position of bed sensors. (b) the single pulse.

Ground truth is needed to evaluate the performance of the proposed pulse rate estimate. It is obtained by a piezoelectric pulse sensor (ADInstruments MLT1010) that is attached to the subject's finger. The ground truth signal is acquired simultaneously through the same ADC for the hydraulic bed sensor, using the same sampling rate to maintain synchronization.

The dataset consists of the measurements from 5 subjects. One subject has a prior cardiac condition. The details of the subjects are listed in Table I. The subjects are asked to lie flat on the back for 2.5 minutes. After the measurement cycle, the data having the strongest amplitude of j-peaks among the four transducers will be kept for further analysis. Fig. 3 (a)

shows a typical signal from one of the hydraulic transducers.

III. METHODOLOGY

We shall model the transducer data as

$$m(t) = r(t) + p(t)\cos(2\pi f_o t) + \varepsilon(t) \quad (1)$$

where $r(t)$ is the respiration cycle which represents a sinusoid with frequency equal to the respiration rate. $p(t)$ is a periodic pulse sequence modeling the j-peak of the BCG with the cycle rate equal to the pulse rate and f_o is the modulation frequency chosen as 4Hz to match the data measurements. $\varepsilon(t)$ is the additive noise. Fig. 2 shows the individual components of (1) and the synthesized signal $m(t)$. Comparing it with the actual signal measurement in Fig. 2 (e), our data model (1) appears to be quite reasonable.

Since the respiration rate is much slower than the pulse rate, the respiration signal $r(t)$ can be removed by applying a band-pass filter to $m(t)$. The filtered data is represented as

$$m'(t) = BPF(m(t)) = p(t)\cos(2\pi f_o t) + \varepsilon'(t). \quad (2)$$

We will need to remove the modulation component $\cos(2\pi f_o t)$ in order to obtain the pulse information. We propose to use the Hilbert transform for this purpose. The Hilbert transform replicates the input signal as the real-part and produces its 90 degree phase shift version as the imaginary component. The Hilbert transform of $m'(t)$ can be expressed as

$$h(t) = m'(t) + jm_i(t). \quad (3)$$

$m_i(t)$ is after 90 degree phase shift of $m'(t)$ and it is approximately equal to

$$m_i(t) \cong p(t)\sin(2\pi f_o t). \quad (4)$$

when the noise is negligible and the variation of $p(t)$ is ignored.

Since we are interested in the period of $p(t)$, the magnitude square of $h(t)$ can remove the unwanted modulation component, giving

$$g(t) = |h(t)|^2 = (m'(t))^2 + (m_i(t))^2 = (p(t))^2 \quad (5)$$

which can be processed further to obtain the pulse rate.

IV. ALGORITHM

Fig. 3 depicts 30 seconds of the data measurement in the time and in the frequency domain. The time domain data appears quite random and the strong peak in the frequency domain represents the respiration rate. Without processing the data carefully, it is not possible to observe the pulse rate.

Fig. 4 shows the block diagram to obtain the pulse rate. We apply a band-pass filter to the data to remove the respiration information. Then we segment the data and apply the Hamming window to remove the leakage in the frequency domain. The Hilbert transform mentioned as above extracts the heart beat envelopes in the data segments.

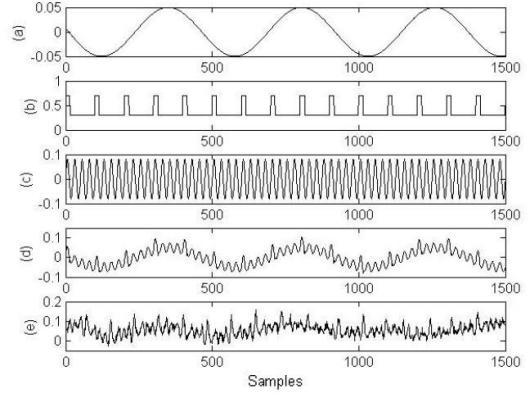


Fig. 2. The modeling of bed sensor data, the x-axis covers 15 sec at 100 Hz sampling rate. (a) the respiration signal $r(t)$. (b) the pulse signal $p(t)$. (c) the frequency component $\cos(2\pi f_o t)$. (d) the data synthesized according to 1 without $\varepsilon(t)$. (e) the measuring data.

Finally, by using the fast Fourier transform (FFT) and finding the first peak location in the frequency domain, we can obtain the pulse rate.

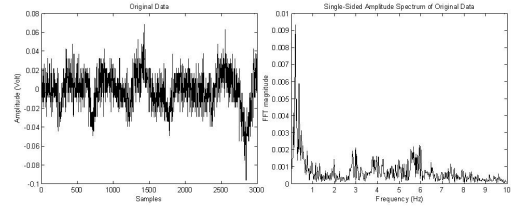


Fig. 3. Thirty seconds of data. (a) the time domain of the data. (b) the frequency domain of the data.



Fig. 4. The data processing blocks for pulse rate estimation.

A. Band-pass Filter

We would like to decouple the respiration information when estimating the pulse rate. In this paper, the Butterworth filter with order equal to 6 is used. The respiration rate is often lower than 0.5 Hz. Therefore, the band-pass filter with cutoff frequency equal to 0.7 Hz to 10 Hz can remove most of the respiration component in the data. The result after band-pass filtering is shown in Fig. 5. Comparing with Fig. 3, it is clear that the pulse information appears on the time domain waveform. Most of the low frequency components in Fig. 3 (b) are gone in Fig. 5 (b) while the information up to 10 Hz is maintained.

B. Sequential Estimation

The size of the moving window for segmentation is equal to 30 sec. After the pulse rate estimation using the data within the window, the window advances 10 sec in time for the next processing segment. The 67% window overlap can

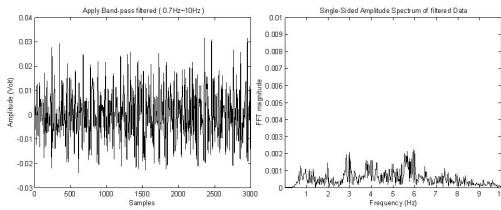


Fig. 5. Data after band-pass filtering. (a) data in the time domain. (b) data in the frequency domain.

prevent any loss of information at the edge of the window. The windowed data for estimation can be represented by

$$\tilde{x}_i(n) = w(n)x(n + i(N/3)) \quad (6)$$

where $\tilde{x}_i(n), i = 0, 1, \dots, N - 1$ denotes the data after segmentation and windowing, i represents the frame number and n represents the sample number within the segment. N is window size and is equal to 3000. $w(n)$ is the window function. It is chosen to be the Hamming window.

Fig. 6 (a) gives the time data signal $\tilde{x}_i(n)$ after the Hamming window. The corresponding frequency domain data is shown in Fig. 6 (b).

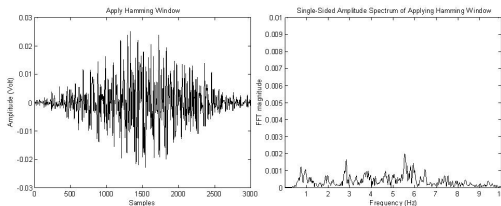


Fig. 6. A data segment after applying the the Hamming window. (a) data in the time domain. (b) data in the frequency domain.

C. Hilbert Transform

In Fig. 6 (b), after band-pass filtering and windowing, the pulse information is still not apparent, due to the modulation harmonic component $\cos(2\pi f_o t)$ that is coupled with the pulse signal $p(t)$. The Hilbert transform will be used to extract the pulse envelopes. After applying the Hilbert transform and magnitude-square by (3) and (5), Fig. 7 (a) shows time domain output. The periodicity in Fig. 7 (a) can be easily observed when taking the FFT and according to the FFT magnitude spectrum shown in Fig. 7 (b), it has a clear and distinctive main peak at the pulse rate which is equal to 0.95 Hz (57 heart beats per min) in this case.

V. RESULTS

Fig. 8 - Fig. 12 show the pulse rate estimation result of the subjects over 2.5 minutes. The open circle denotes the result from the proposed method and the close circle represents the ground truth. It is noticed that the pulse rate of subject 1 changes significantly. Nevertheless, the proposed method is able to follow and provide reasonably good estimation. To better characterize the performance, we compute the error rate defined as

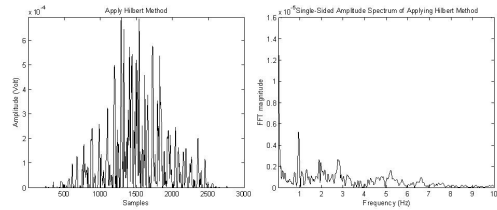


Fig. 7. Signal after applying the Hilbert transform and magnitude square to the windowed data segment. (a) the time domain signal. (b) the FFT magnitude of (a).

TABLE II

ERROR RATE OF TWO METHODS.

Subject	Proposed method	WPPD
1	0.96 %	0.76 %
2	0.85 %	1.17 %
3	0.46 %	2.08 %
4	0.33 %	1.88 %
5	0.60 %	2.08 %

$$Error\ Rate = \frac{1}{M} \cdot \sum_{i=1}^M \frac{|GT(i) - Est(i)|}{GT(i)} \times 100\ % \quad (7)$$

where $GT(i)$ is the ground truth, $Est(i)$ is the estimated pulse rate at segment i and M is the total number of segments. $GT(i)$ is obtained by applying FFT on the i th segment in the piezoelectric pulse sensor data and locating the largest peak in the frequency domain. The results are shown in Table II.

Subject 4 has lowest error rate equal to 0.33 % and subject 1 has highest error rate equal to 0.96%.

Table II also provides the results for the method from [11] [12] for comparison, which used the windowed peak to peak (WPPD) method to analyze the data in the time domain. The proposed algorithm gives much better results in subjects 2 to 5. For subject 1, we have a little bit worse result than the WPPD method.

Comparing the estimation results of subject 1 in Fig 8 with that of subject 4 in Fig 11, subject 1 has larger pulse rate variations. Because the proposed method obtains the pulse rate through sliding window which assumes the pulse rate is constant within a segment, the high variations of pulse rate will increase the error rate. In addition, the time domain of sensor data for subject 1 is cleaner than for subject 4. Therefore, the WPPD has lower error rate for subject 1. On the contrary, the new algorithm performs well for all five subjects. Improving the performance of the proposed method under high variations in pulse rate is a subject for further study.

VI. CONCLUSIONS

In this paper, we propose a new algorithm to obtain the pulse rate from a hydraulic bed sensor. The transducer data contains the respiration information and the multi-peak BCG. A band-pass filter is used to remove the respiration information. The Hamming window is applied to reduce the

leakage in the frequency domain due to data segmentation. By exploiting the Hilbert transform, we can extract the pulse envelopes and obtain accurate pulse rate estimate in the frequency domain. Comparing with WPPD, the new algorithm has a lower error rate when the pulse rate is not changing rapidly. In the situation when the pulse rate variation is high, reducing the window size could improve the performance. We plan to study about how the subject posture and body movement affect the measurement signal quality, consistency and the performance of the proposed method.

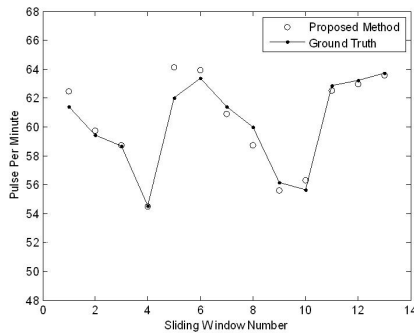


Fig. 8. The pulse rate estimation result of the proposed method and ground truth for subject 1.

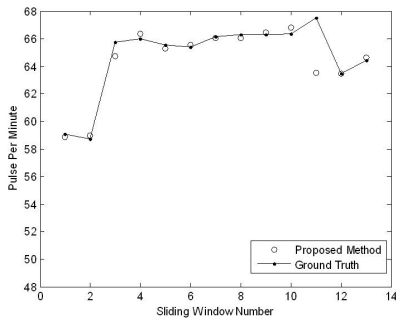


Fig. 9. The pulse rate estimation result of the proposed method and ground truth for subject 2.

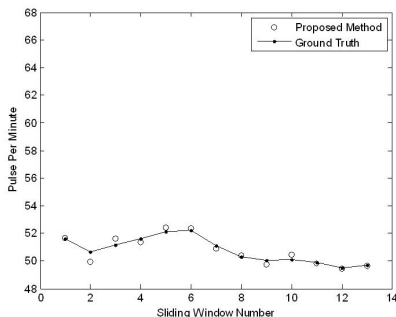


Fig. 10. The pulse rate estimation result of the proposed method and ground truth for subject 3.

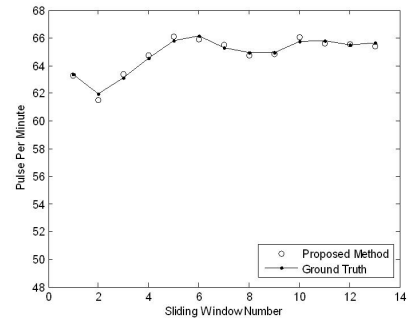


Fig. 11. The pulse rate estimation result of the proposed method and ground truth for subject 4.

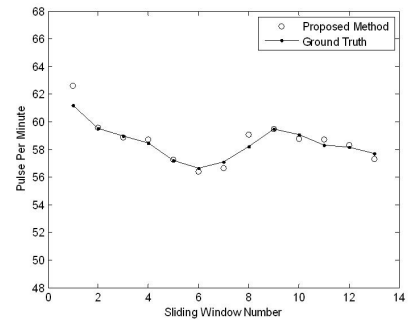


Fig. 12. The pulse rate estimation result of the proposed method and ground truth for subject 5.

REFERENCES

- [1] P. A. Heidenreich *et al.*, "Forecasting the future of cardiovascular disease in the United States: a policy statement from American Heart Association," *Circulation*, vol. 123, pp. 933-944, 2011.
- [2] K. Nakajima, A. Osa, S. Kasaoka, K. Nakashima, T. Maekawa, T. Tamura, and H. Miike, "Detection of physiological parameters without any physical constraints in bed using sequential image processing," *Jap. J. Appl. Physics*, vol. 35, pp. 269-272, 1996.
- [3] K. Mukai, Y. Yonezawa, H. Ogawa, H. Maki, and W. M. Caldwell, "A remote monitoring of bed patient cardiac vibration, respiration and movement," in *Proc. 31th Annu. Int. IEEE EMBS Conf.*, 2009, pp. 5191-5194.
- [4] Y. Yamana, S. Tsukamoto, K. Mukai, H. Maki, H. Ogawa, and Y. Yonezawa, "A sensor for monitoring pulse rate, respiration rhythm, and body movement in bed," in *Proc. 33th Annu. Int. IEEE EMBS Conf.*, Boston, Massachusetts, 2011, pp. 5323-5326.
- [5] J. H. Shin, Y. J. Chee, D. U. Jeong, and K. S. Park, "Nonconstraint sleep monitoring system and algorithms using air-mattress with balancing tube method," *IEEE Trans. Inf. Tech. in Biomed.*, vol. 14, no. 1, pp. 147-156, 2010.
- [6] H. Maki, H. Ogawa, S. Tsukamoto, Y. Yonezawa, and W. M. Caldwell, "A system for monitoring cardiac vibration, respiration, and body movement in bed using an infrared," in *Proc. 32th Annu. Int. IEEE EMBS Conf.*, 2010, pp. 5197-5200.
- [7] X. Zhu, W. Chen, T. Nemoto, Y. Kanemitsu, K. Kitamura, K. Yamakoshi, and D. Wei, "Real-time monitoring of respiration rhythm and pulse rate during sleep," *IEEE Trans. Biomed. Eng.*, vol. 53, no. 12, pp. 2553-2563, 2006.
- [8] E. Pinheiro, O. Postolache, and P. Girao, "Theory and developments in an unobtrusive cardiovascular system representation: ballistocardiography," *Open Biomed Eng J.*, pp. 201-216, 2010.
- [9] J. G. Proakis and D. G. Manolakis, *Digital Signal Processing Principles, Algorithms, and Applications*, 4th ed, NJ: Prentice-Hall, pp. 693-699.
- [10] A. D. Poularikas, *The transforms and applications handbook*, CRC Press, 1996, pp. 464-486.
- [11] D. Heise, L. Rosales, and M. Skubic, "Refinement and evaluation of a hydraulic bed sensor," in *Proc. 33th Annu. Int. IEEE EMBS Conf.*, Boston, Massachusetts, 2011, pp. 4356-4360.
- [12] L. Rosales, "Exploring passive heartbeat detection using a hydraulic bed sensor system," M.S. thesis, Dept. Electrical and Computer Eng., Univ. of Missouri-Columbia, MO, 2011.